International Forum on Aeroelasticity and Structural Dynamics
IFASD 2024
17-21 June 2024, The Hague, The Netherlands

MULTIDISCIPLINARY DESIGN OPTIMISATION OF AN AIRCRAFT WITH THE SEMI-AEROELASTIC HINGE DEVICE

Marta Colella[1], Mario Peinado García[1], Francesco Saltari[1], Franco Mastroddi[1], Fabio Vetrano[2], Paolo Mastracci[3], Andrea Castrichini[3]

[1]Dept. of Mechanical and Aerospace Engineering
Sapienza University of Rome
Via Eudossiana 18, 00184 Rome, Italy

[2]Airbus Operations S.A.S., 31060 Toulouse, France

[3]Airbus Operations, Ltd., Filton, England BS99 7AR, United Kingdom

Keywords: Multi-disciplinary design optimisation, static aeroelasticity, semi-aeroelastic hinge, folding wingtip

Abstract: This paper presents a multidisciplinary design optimisation approach aimed at improving aircraft performance by incorporating the semi-aeroelastic hinge (SAH) device onto the wings. Such a technology is an enabler for higher aspect ratio wings with less induced drag and little increase in wing weight, whilst also meeting airport gate limitations. The paper focuses on the optimisation of a single-aisle aircraft to ensure that the internal wingspan remains below the maximum range to classify the aircraft as Category C. Trim, manoeuvre, aileron reversal and roll analyses are used to set the constraints on the aircraft, while the performance model is used to evaluate the range set as the objective of the optimisation. The performance of the aircraft with the semi-aeroelastic hinge device is compared against an aircraft with no wingtip extension and the so-called folding wingtip model, where the wingtips are only used on the ground.

1 INTRODUCTION

Different emerging technologies are currently under investigation in the aerospace industry with the goal of achieving net zero greenhouse emissions by 2050. This is expected to be achieved by the progressive introduction of sustainable aviation fuel (SAF) and the development of new aircraft designs, with a significant focus and research endeavours on the exploration and development of new materials and innovative wing-design concepts.

Lift-induced drag is a significant portion of the overall drag, which can be reduced by increasing the wingspan. Nevertheless, this increase is limited by the maximum aircraft span permitted at airports, as well as an increase in wing internal loads that is affected by the rise of the bending moment. The Folding WingTip (FWT) concept is a solution that is gaining ground in view of the limited space available at airports, where the wing, which is limited in size in relation to a given airport category, is equipped with a wingtip that provides a wing extension during take-off and flight therefore enhancing the lift-to-drag ratio, but folds up on the ground, allowing the aircraft to fit into the specific aircraft category ramp. This solution design has been extensively used for carrier-borne aircraft, and has been also implemented by Boeing in the new B-777X [1]. Conversely, this solution results in increased bending moments causing aircraft structural design to provide increased wing weight to maintain the stress below the safety threshold. On the other

hand, in the SAH concept the wingtips are also exploited in flight as loads alleviation device thus allowing to reduce the wing-induced drag reduction while ensuring a negligible increase in the wing-box structural sizing [2]. A picture showing the main differences between these two concepts is displayed in Fig.1.

Recent research [3–6] has focused on investigating the advantages of utilising a flexible wing-fold device for loads alleviation and exploring its potential use on civilian jet aircraft. It was shown that the orientation of the hinge line relative to the airflow is a key parameter to enable successful load alleviation. This effect helps to decrease the loads on the wing, making it possible to extend the wingtip without significantly increasing the overall weight of the wing. Flared hinge devices have been found to be the most suitable option for both ground and flight uses. Prior research showed that a floating wingtip is essential for optimising the load alleviation performance [3]. Nevertheless, the absence of hinge stiffness in the wingtip can result in the onset of deflection during a straight and level cruise flight due to static trim loads. Moreover, the presence of unsteady aerodynamic loads can give rise to the occurrence of continuous oscillating motion. These deflections and motions are undesired as impact negatively on aerodynamic performance and causing potentially undesired rigid-body dynamic motion. Thus, ideally, the wingtip should remain stable not deflecting during cruise flight but only release itself when encountering gusts. This concept, known as a SAH, involves a dedicated mechanism to keep the wingtip in place during cruise. When a gust is detected, the mechanism releases the wingtip, allowing it to act as a load alleviation system driven by the aerodynamic and the inertial forces. After the load event is finished, an actuator is then engaged to bring back the wingtip to the original configuration. Furthermore, research has been conducted on double-hinge configurations [7–12]. In this case, both hinges were oriented along the longitudinal axis of the aircraft, allowing a significant variation of the wingspan during flight, and increasing the aircraft manoeuvrability.

Previous research examined how the Semi-Aeroelastic Hinge (SAH) in a standard commercial jet aircraft affect loads, flutter stability, and handling qualities using a linear aeroelastic model and assuming minimal wingtips deflection. However, numerical findings demonstrated that the wingtips could actually reach angles exceeding 45 degrees, prompting the question of whether a linear aeroelastic model is suitable for accurately modelling the behaviour of floating wingtips. To address such a limitation, Conti et Al. [13] introduced a non-linear static formulation. It was shown that, in the presence of a side slip angle, the static response of the floating tips is driven by the effective flare angle which is the combination of the structural hinge flare angle and the flow side slip. Mastracci et Al. [14] extended these studies including also nonlinear dynamic effects, thus allowing to investigate the nonlinear post flutter response for different design parameters and flow conditions. These studies confirmed that the hinge line angle relative to the incoming flow, is a key parameter for achieving a successful load alleviation.

None of the SAH related studies currently present in the literature have explored its impact on aircraft design and performance through methodological preliminary design optimisation. This work exploits an in-house developed multi-disciplinary optimisation environment to provide aircraft optimisation with semi-aeroelastic hinges. Specifically, the aircraft geometry (i.e. wing and tail area) is optimised while sizing the structural elements to meet the requirements of trimmability and safe manoeuvrability. The approach starts by selecting a specific class of aircraft with an assigned fuselage whose mass and inertial properties (considering the payload) are considered fixed. The wing surfaces are therefore optimised, maximising the mileage range while maintaining the requirement of the aircraft to be of airport category C (Ref. [15]), *i.e.*

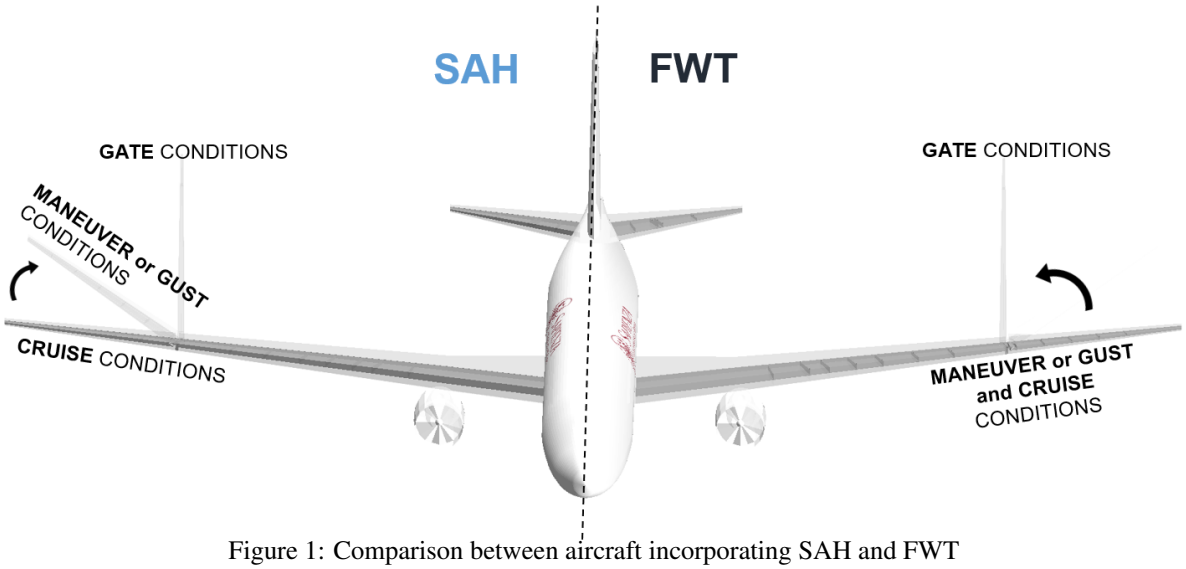

Figure 1: Comparison between aircraft incorporating SAH and FWT

with a maximum wingspan of 36 m while on the ground. Three aircraft types are optimised in order to assess the increase in performance introduced by the SAH against the more classical configurations: *a)* aircraft without any wingtip, *b)* the aircraft with the folding wingtip and *c)* the aircraft with the semi-aeroelastic hinge device.

The paper is organised as it follows. Sec. 2 provides the introduction of the optimisation strategy, Sec. 3 provides an overview of the aeroelastic modelling, while Sec. 4 provides the results of the different optimisation. Finally a concluding remarks ends the paper.

2 OPTIMISATION METHODOLOGY

The Multidisciplinary Design Optimisation (MDO) involves finding the optimal design solution, aligning with specific goals and satisfying target constraints. In the aeronautical field, these goals are often focused on improving the aircraft performance, such as increasing aerodynamic efficiency or reducing gross weight. Exploring innovative designs or refining existing ones is a common application of this process.

This article presents an optimisation procedure for the preliminary design phase of aircraft with the SAH, taking into account also the current certification requirements. The set goal consists in sizing the wing, tail, and aileron to maximise the aircraft range on a fixed amount of fuel, accounting for structural, aeroelastic, and control constraints. More specifically, the objective function, hereafter mileage range, is calculated using the Breguet formula for jet aircraft for performance at constant cruise speed U_∞, lift c_L and drag c_D coefficients, Ref. [16]

$$R = \frac{U_\infty}{SFCJ}\,\frac{c_L}{c_D}\,ln\frac{W\big|_{MTOW}}{W\big|_{MTOW} - W_f} \tag{1}$$

in which the $SFCJ$ is the thrust-specific fuel consumption, while W is the weight evaluated at the take off condition and W_f is the weight of the fuel stowed. Different design provides different aircraft weight as well as flight conditions used for the performance evaluation. More specifically, once the Mach number M_∞ is given, the flight condition (in terms of dynamic pressure) considered for the evaluation of the objective function is the one presenting the higher lift-to-drag ratio L/D_{max} (see Fig. 2).

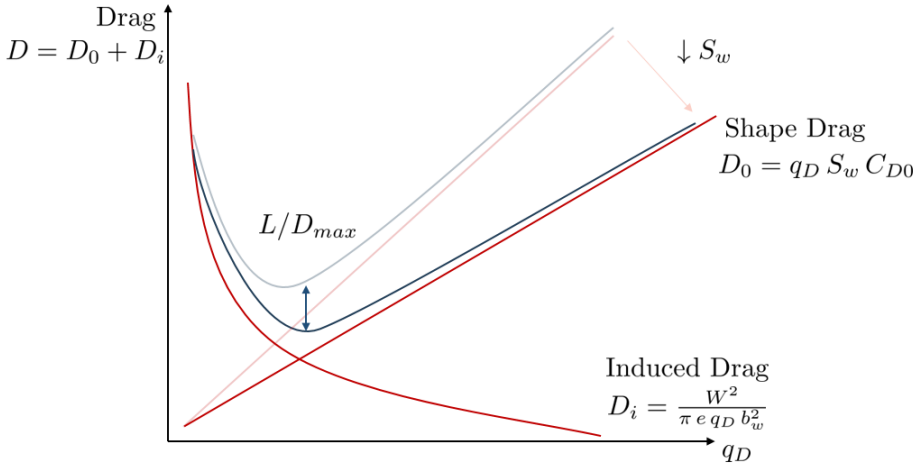

Figure 2: Best performance definition: L/D_{max} and D_{min}

The optimisation problem involves objectives and constraints that are sensitive to both structural and aerodynamic variables. A total number of 49 design variables, classified in structural and aerodynamics variables in Tab. 1, are considered to account for the different aircraft design. In detail, structural design variable set includes the thickness of the different 2D structural elements as well as the spar caps area, whereas the aerodynamic variable set include all those parameters that allow to sketch the wing platform. Since accounting for a category C aircraft, the maximum span of the inner wing is fixed at 36 m, while, in the optimisation in which the wingtip is present - either FWT or SAH -, the wingtip span is set a design variable, probably the most interesting one. The flare angle is a parameter that does not affects the static aeroelastic response and therefore, it is set equal to $15\,deg$ for all the design.

The proposed methodology employs static aeroelastic analyses, selecting a manifold of the aircraft most critical flight conditions summarised in Tab. 2. Trim and manoeuvre analyses provides the optimisation with the constraints set on the maximum stress as well as the angle of attack and maximum control surface deflections. Furthermore, the analyses include the assessments of the ailerons effectiveness, in terms of control reversal speed and rolling time and the assessment of the rigid body stability.

The design of the aircraft with the SAH requires the analyses to be performed in both configurations the aircraft may operate during flight: *i)* the configuration in which the wingtips are extended and locked (LSAH, Locked Semi-Aeroelastic Hinge), *ii)* the configuration in which the SAH are free to flap (FSAH). The FSAH configuration is used in those manoeuvres requiring high load factor (or intense gusts), whereas the LSAH is the configuration in which the aircraft operates for the majority of the flight, enhancing lift-to-drag ratio and where the performance of the aircraft is evaluated in terms of mileage range.

Therefore, the identification of the most critical conditions in terms of loads and manoeuvrability is a crucial aspect for both FSAH and LSAH configurations. Since the semi-aeroelastic hinge is employed to reduce loads, the higher load factor scenarios are identified for the FSAH configuration. Additionally, as the inner wing surface is the only effective wing surface in FSAH, this configuration will also be the most critical for evaluating the manoeuvrability of the aircraft. Furthermore, it is necessary for the aircraft to be capable of performing lower load factor manoeuvres even in the LSAH configuration. This is to prevent the hinge from being

continuously used, which could result in overload and fatigue of the hinge and actuator system. Additionally, it allows for the consideration of potential failures of the hinge/actuator system, enabling low-g manoeuvres to facilitate re-entry and landing. Therefore, a Loads Reduction Factor (LRF) is introduced to reduce the maximum permissible load in LSAH configuration with respect to the one expressed in the certification requirements. As an example, the flight envelope of the Maximum Take Off Weight (MTOW) condition is provided in Fig. 3. The abscissa of the flight envelope is provided in dynamic pressure, that, can be translated in terms of altitude when considering a fixed Mach value.

In more specific terms, the overall flight envelope (enclosed by a dashed yellow line) is defined as the area of intersection between the flight envelopes of the LSAH and FSAH configurations, respectively delineated by the pink and blue solid lines in Fig. 3. The lines labelled $\mathrm{A}-\mathrm{B}$ for LSAH and $\bar{\mathrm{A}}-\bar{\mathrm{B}}$ for FSAH define the margin of manoeuvrability at which, for lower dynamic pressures, the aircraft will encounter a stall. The slope of these curves is dependent upon the effective lifting surface, which, for the FSAH configuration, is lower due to the wingtip generating less lift when flapping. The ordinate values at B and $\bar{\mathrm{B}}$ defines the maximum loads factor for LSAH and FSAH, respectively. The design implies that FSAH configuration allows manoeuvres at $2.5g$, while, as a consequence of the introduction of the loads reduction factor, the LSAH configuration is allowed to manoeuvre up to $2.5/LRFg$.

This results in a region of loss of manoeuvrability (red area) compared to standard flight envelope diagrams because the LSAH configuration performs aerodynamically but not structurally, while FSAH performs structurally but not aerodynamically. This poses critical challenge for the choice of dynamic cruise pressure, which should coincide with the aircraft best performance dynamic pressure. In fact, the optimal flight point for the LSAH configuration is typically situated below the red zone (point C). In this study, it is assumed that the cruise coincides with the optimal performance value. This is currently not aligned with the CS25 requirement since the aircraft would be able to achieve $2.5/LRFg$ and not a $2.5g$ manoeuvre at that dynamic pressure. A potential solution to this issue would be to reduce the LRF value, although this may result in a reduction in the benefits introduced by the SAH.

The aircraft optimisation presented in this works assumes $LRF = 1.5$. Notice that, given the imposed analyses and constraints, the optimisation algorithm will tend to size the structural element and wingtip span in order to meet the safety margin for both FSAH and LSAH given the enhanced bending moment provided by a longer wing. The aircraft with FWT can be considered as a limit case of aircraft with SAH in which LRF tends to 1. Therefore, the same constraints are set for the manoeuvrability at $12000m$ of altitude.

The optimisation process, which utilises the aforementioned design variables, constraints and objectives, is illustrated in the Fig. 4. An initial guess, which is typically generated through random algorithms, serves as the initial starting point for the optimisation process. For each individual within the optimisation, the aeroelastic model and the set of aeroelastic and performance analyses are defined. The optimisation algorithm chosen is the *Multi-Objective Genetic Algorithm* (*MOGA-II*) [17, 18]. More specifically, this algorithm uses a multi-search elitism for robustness, while for a faster convergence exploits the directional crossover, observing the objective function of different individuals. Even thought it is an algorithm mainly designed for the optimisation of *Multi-objective* problems, it results to be effective also in solving *Single-Objective* optimisations [19].

		Wing	Tail	Aileron
Structural	Skin panels	thickness	thickness	—
	Spars	web thickness	web thickness	—
		cap areas	cap areas	—
	Ribs	number	number	—
		thickness	thickness	—
Aerodynamic	Angles	sweep	—	—
	Length	root chord	root chord	chord
		taper ratio	taper ratio	—
		SAH span	span	span
	Position	—	—	position

Table 1: Design Variables definition

	Disciplinary constraints		
Analyses	Structural	Aeroelastic	Control
TRIM	Maximum Stress	Angle of Attack HTP Angle	
MANOEUVRE	Maximum Stress	Angle of Attack Elevator Angle	Pitching time
AILERON RESPONSE	Maximum Stress	Reversal speed	Rolling time
RIGID BODY STABILITY		Damping positiveness	

Table 2: Disciplinary Constraints

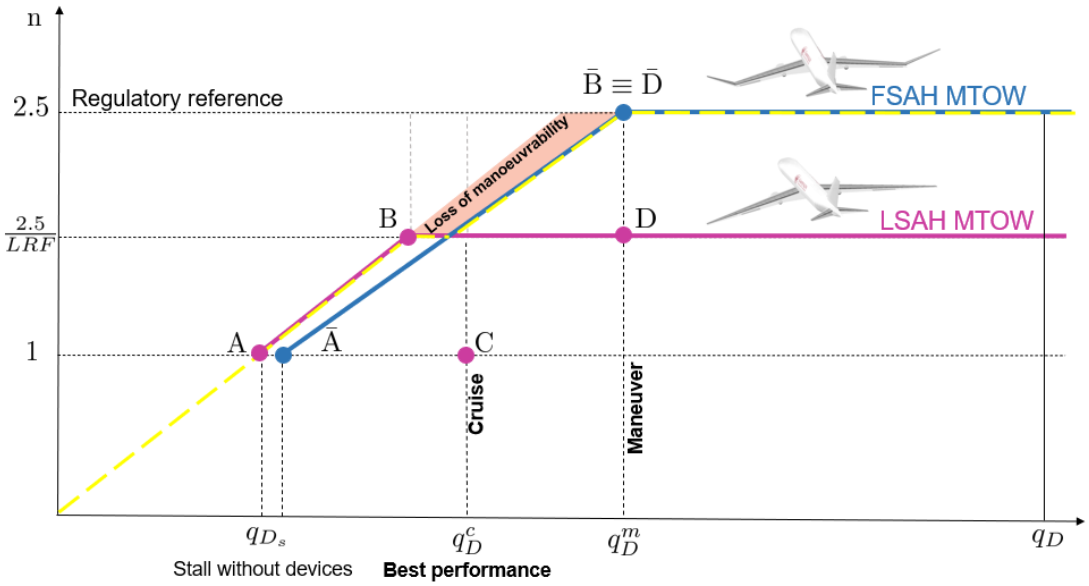

Figure 3: Flight envelope: critical points for LSAH and FSAH

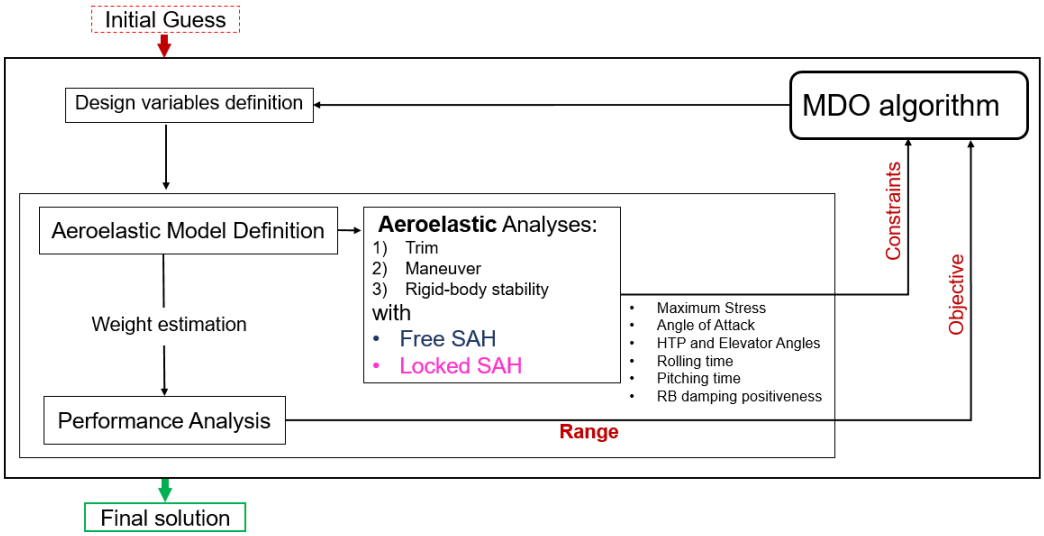

Figure 4: The optimisation process

3 AEROELASTIC MODELLING

Leveraging between accuracy and computational efficiency is a crucial aspect in optimisation processes. In this regard, the use of off-the shelf aeroelastic models like NASTRAN models provides a good balance between the rapid exploration of objective and constraints and the descriptive accuracy of the physical problem. This section summarises the features of the model generation environment used to provide MSC-NASTRAN® with the Finite Element Method (FEM) model of the structure and the Doublet Lattice Method (DLM) model of the steady aerodynamics (Ref. [20]).

The model generator exploits a parametric approach to build the aircraft finite element model handling both structural and geometric variables. More specifically, the FEM model includes the wing and the horizontal tail, neglecting the detailed modelling of the fuselage and engines assumed as a concentrated mass element. Both the wing and tail are described via shell and bar elements with variable properties along the span able to model the behaviour of the wing box structure. The amount of stowed fuel and the payload to be transported are considered as fixed parameters, here modelled again as concentrated mass. Moreover, the model generator provides the actuators via concentrated mass with mass values depending on the size of the control surfaces and a distribution of leading edge, centre box, and trailing edge masses in accordance with the approach outlined in Ref. [21]. The semi-aeroelastic hinge (see Fig. 6) is modelled via two spherical joints (RJOINT elements) passing by two pairs of node (A-B and C-D) defining the hinge line that are connected with rigid-body element to the wing box nodes, allowing free rotation of the wingtip about the hinge. The size of the wingtip determines the mass of the hinge actuator to restore the wingtip in its locked position. Additionally, rotational springs between the nodes A-B and C-D provide rotational stiffness that is about zero in the FSAH configuration and high in the LSAH configuration.

On the other hand, the aerodynamic wing and tail lifting surfaces are modelled using a DLM model, where each macro element is modelled to provide optimal non-equally distributed chord-wise discretisation of the pressure load, while preventing the mesh element from assuming higher aspect ratios. A fixed percentage of the tail chord is allocated to the elevator, which is modelled as an aerodynamic control surface and used during manoeuvres, while the entire tail

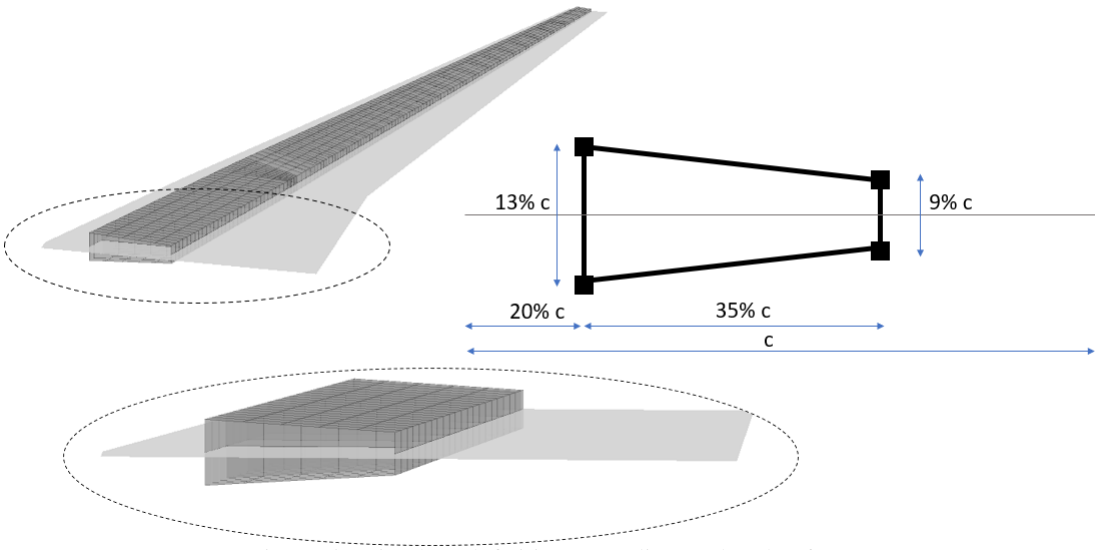

Figure 5: Wing box definition according to the plan form

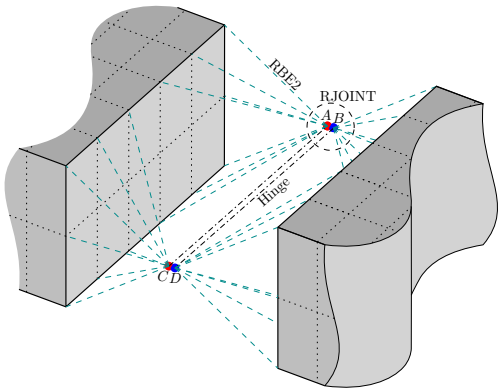

Figure 6: SAH Structural Definition

surface is allowed to rotate to balance the aerodynamic forces during trim analyses. On the other hand, the aileron control surface is modelled according to the dedicated design variables, namely the aileron/wing surface ratio and the position with respect to the wing. Aero-structural coupling is performed using an approach involving fish-bone non-structural nodes and surface spline (SPLINE1).

4 RESULTS

The objective of the analysis is to optimise a single-aisle aircraft flying at Mach $M_\infty = 0.77$ with a maximum capacity of 170 passengers and the ability to stow 18 tons of fuel. Additionally, the inner wing span is prescribed to a maximum of 36 m, allowing the aircraft to be taxied into Category C airport ramps, thereby reducing operational costs. A comparative analysis is employed to evaluate the semi-aeroelastic hinge device effectiveness in enhancing aircraft performance. This analysis is conducted across three configurations: tip-less, folding wingtips and semi-aeroelastic hinge. Indeed, by considering modelling uncertainties impacting equally the performance evaluation of the three configurations, the approach enables the quantification of the performance improvement conferred by SAH in comparison to the tip-less and FWT configurations.

4.1 Tip-less aircraft

Tip-less aircraft optimisation considers the analysis constraints given by certification requirements considering, as example, the maximum load factor equal to $n_z^{max} = 2.5$. Figure 7 shows the evolution of the objective function, *i.e.* the range, as a function of the number of iteration. Unfeasible configurations are displayed in grey, while feasible ones are shaded in blue according to aircraft design take-off weight. The range $\bar{R}$ and weight $\bar{W}$ are normalised with respect to the values assumed by the best design, *i.e.*, R^{REF} and W^{REF} hereafter assumed as reference also for the design of the aircraft with FWT and SAH devices.

Through the optimisation process, the mileage range increases from a starting value of roughly 6000 km to the maximum value $R^{REF} = 6503$ km (corresponding to $\bar{R} = 1$), providing an improvement of 8.4% of the objective. The maximum take-off weight associated to the best design is $W^{REF} = 64.4$ tons. More in detail, the geometry of the optimised reference aircraft is displayed in Figure 8, whereas its main characteristics are listed in Table 3 and performance listed in Tab.3.

	REFERENCE			FWT			SAH		
	Wing	Tail	Aileron	Wing	Tail	Aileron	Wing	Tail	Aileron
Surface	119.79 m^2	23.14 m^2	1.40 m^2	155.86 m^2	30.26 m^2	2.78 m^2	156.6 m^2	28.14 m^2	3.01 m^2
Span	36 m	12.28 m	2.95 m	51.06 m	11.11 m	3.30 m	51.24 m	12.72 m	4.66 m

Table 3: Reference parameters: tip-less, FWT and SAH configuration

4.2 Aircraft with Folding Wingtip device

As mentioned in Sec. 2, the aircraft with in ground folding wingtip represents the limit case of design when imposing unitary LRF. Figure 9 provides the trend of the objective function as a function of the number of iteration. Notice that the range and weight are normalised with respect to the value assumed by the tip-less configuration. Figure 10(a) shows the comparison between the optimised tip-less aircraft and the aircraft with FWT whereas 10(b) provides the an example of the aircraft deformation and stress distribution, σ at $n_z = 2.5$. Table 3 lists the geometrical

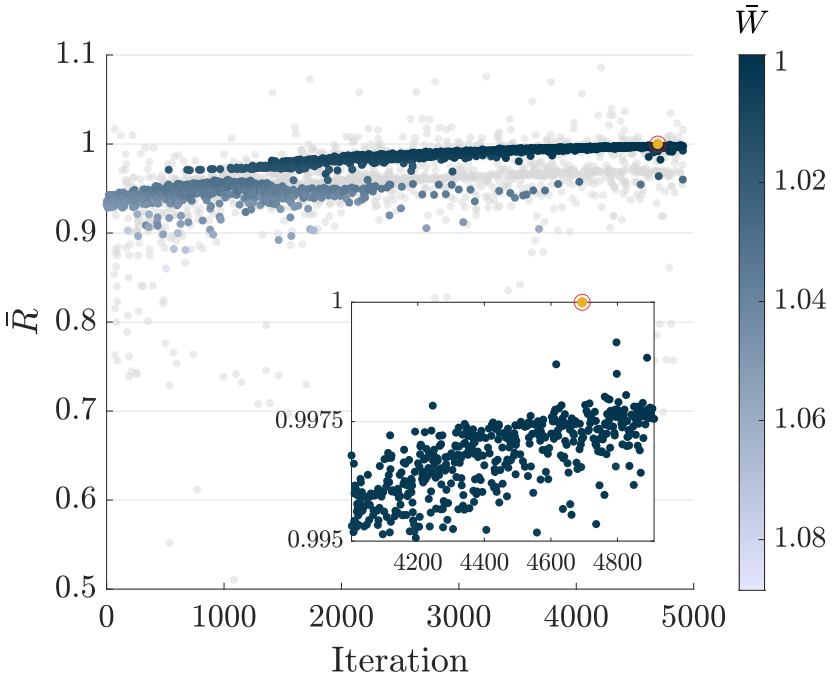

Figure 7: Objective function history: tip-less aircraft

DESIGN FEATURES	REFERENCE	FWT	SAH
Range	6486 km	7839 km	8055 km
Lift-to-Drag ratio	12.34	16.24	16.41
Weight	64431 kg	69458 kg	68297 kg
Aspect Ratio	10.82	16.72	16.76
Rolling Time	8.44 s	7.72 s	*LSAH:* 7.88 s *FSAH:* 7 s

Table 4: Performance of the optimised tip-less aircraft, FWT configuration and SAH configuration

features of the best aircraft design with FWT, whereas its performance are summarised in Tab. 3.

Table 3 provides that the maximum obtained range corresponds to 7871 km, representing a 21% increment with respect to the optimal tip-less aircraft stowing the same amount of fuel. The take-off weight increases by a 7.8% with respect to the reference, that is, about 69.5 tons. This is due an overall increase of 41% of wing span influencing both the litf-to-drag ratio and the mass of the aircraft. The rolling time is still close to the optimised tip-less aircraft, that is 7.72 s, due mainly to the noticeable increase in the aileron surface.

4.3 Aircraft with Semi-Aeroelastic Hinges

The inclusion of SAH aims at extending the wingspan reducing the lift-induced drag while saving the aircraft overall mass. This is obtained at the cost of releasing the hinge during the flight to allow the aircraft to face high vertical load manoeuvres and gusts. The optimisation is conducted using the approach outlined in Sec. 2. Figure 11 provides the objective function evolution as a function of the number of iterations. The geometry of the best aircraft design is shown in Figure 12 whereas the an example of the manoeuvre aeroelastic response in both FSAH and LSAH configurations are displayed in Fig. 13 in which the normal load factor is $n_z = 2.5$ and $n_z = 1.66$, respectively. Notice that the maximum costing angle observed in the

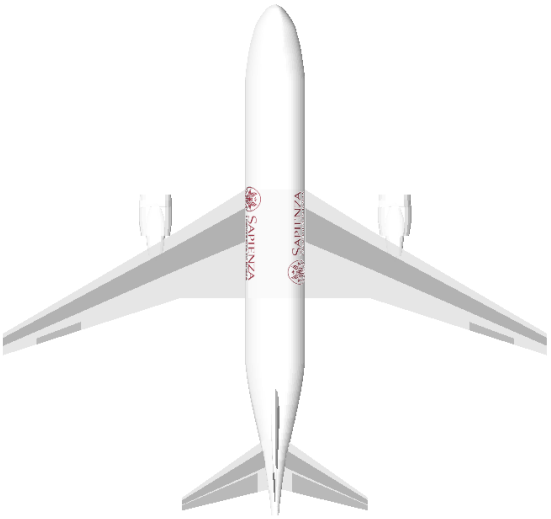

Figure 8: Reference Geometry: tip-less configuration

present manoeuvre analysis is $53.4\,deg$.

Comparing Table 3, the inclusion of the SAH devices enables an increase of the maximum mileage range from 6486 km to 8055 km, representing a 24% relative increment with respect to the tip-less best design and about 3% with respect to the aircraft with FWT. Additionally, it can be seen that both the wingspan and the weight increases 43% and 6%, with respect to the reference and FWT configurations respectively. The SAH aircraft has a higher wet surface with respect to the tip-less reference geometry (156.6 m^2 and 119.79 m^2 respectively) , thus leading to a higher viscous drag contribution. However, the higher aspect ratio of the SAH aircraft allows to significantly reduce the induced drag component allowing a total drag reduction and thus longer range.

Furthermore, the aircraft incorporating SAH provides higher rolling capabilities with respect to both tip-less and FWT aircraft. In particular, the LSAH configuration presents a rolling time equal to 7.88 s while the FSAH configuration presents a rolling time of 7 s. The maximum take-off weight of the vehicle with SAH presents a reduction of 1.7% with respect to the aircraft with FWT.

5 CONCLUSION

This study introduced an innovative multidisciplinary design optimisation methodology aimed at enhancing aircraft performance through the integration of a semi-aeroelastic hinge device within the wings. This technology enabled an extension of the wingspan, leading to a consequent reduction in lift-induced drag, while ensuring that manoeuvre and gust-induced loads remained within safe thresholds. The research focused on optimising a single-aisle aircraft to ensure compliance with Category C classification for airport taxiing, with constraints set by trim, manoeuvre, aileron reversal, and roll analyses. The performance model evaluated the range as the optimisation objective. A comparative analysis was conducted between the aircraft equipped with the semi-aeroelastic hinge device, a single-aisle aircraft without outboard wings, and the folding wingtip model, where wingtips were folded solely during airport ground operations. This study underlined the efficacy of incorporating the semi-aeroelastic hinge device in improving aircraft performance while meeting regulatory requirements. It is important to point out that the use of the SAH introduces also a loss in aircraft manoeuvrability when

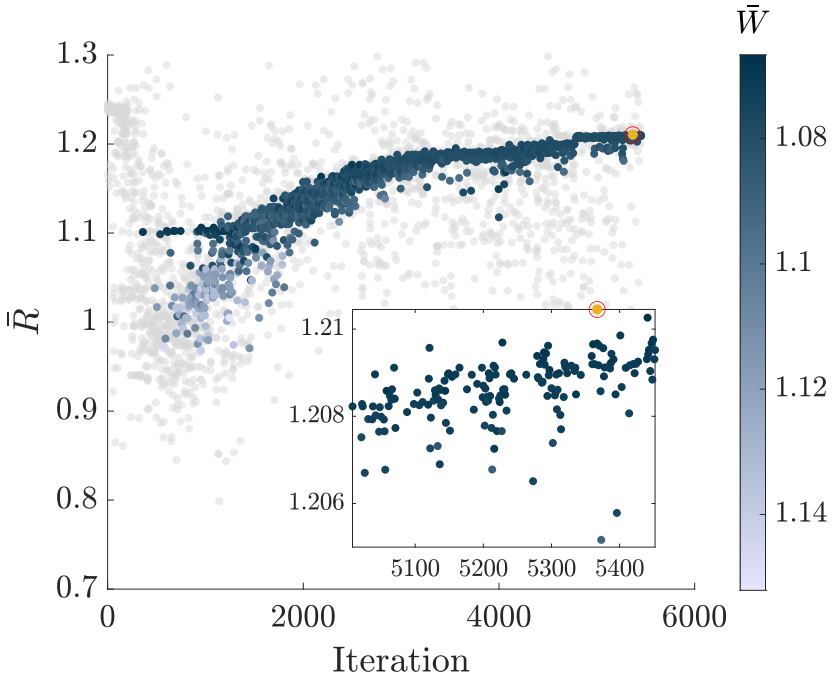

Figure 9: Objective function history: FWT Configuration

compared against the FWT configuration which should be addressed in future works. It was observed that the utilisation of SAH technology in a single-aisle aircraft resulted in an increase of approximately 3% in the aircraft efficiency in comparison to FWT technology.

6 REFERENCES

[1] Boeing. Boeing 777x by design. `https://www.boeing.com/commercial/777x/by-design#tabs-0d30548d49-item-f6863deeff-tab`.

[2] Wilson, T., Azabal, A., Castrichini, A., et al. (2016). Aeroelastic behaviour of hinged wing tips.

[3] Castrichini, A., Siddaramaiah, V. H., Calderon, D., et al. (2017). Preliminary investigation of use of flexible folding wing tips for static and dynamic load alleviation. *The Aeronautical Journal*, 121(1235), 73–94.

[4] Castrichini, A., Cooper, J. E., Wilson, T., et al. (2017). Nonlinear negative stiffness wingtip spring device for gust loads alleviation. *Journal of Aircraft*, 54(2), 627–641.

[5] Castrichini, A., Hodigere Siddaramaiah, V., Calderon, D., et al. (2016). Nonlinear folding wing tips for gust loads alleviation. *Journal of Aircraft*, 53(5), 1391–1399.

[6] Castrichini, A., Wilson, T., Saltari, F., et al. (2020). Aeroelastics flight dynamics coupling effects of the semi-aeroelastic hinge device. *Journal of Aircraft*, 57(2), 333–341.

[7] Tang, D. and Dowell, E. H. (2008). Theoretical and experimental aeroelastic study for folding wing structures. *Journal of Aircraft*, 45(4), 1136–1147.

[8] Snyder, M. P., Sanders, B., Eastep, F. E., et al. (2009). Vibration and flutter characteristics of a folding wing. *Journal of Aircraft*, 46(3), 791–799.

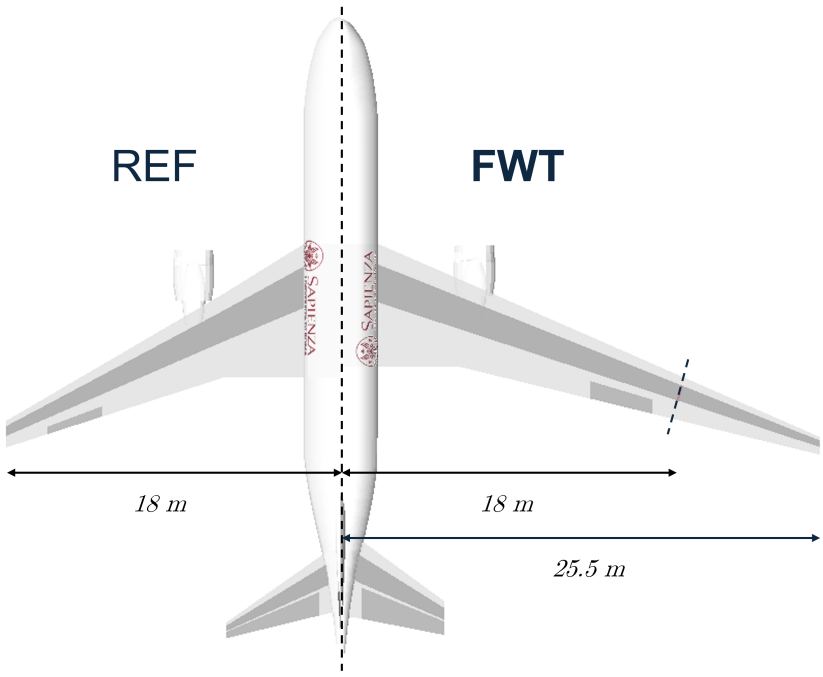

(a) Comparison with tip-less aircraft

(b) Maneuver wing deformation and stress distribution at $q_D = 8.023\,kPa$ and $n_z = 2.5$.

Figure 10: Aircraft with FWT.

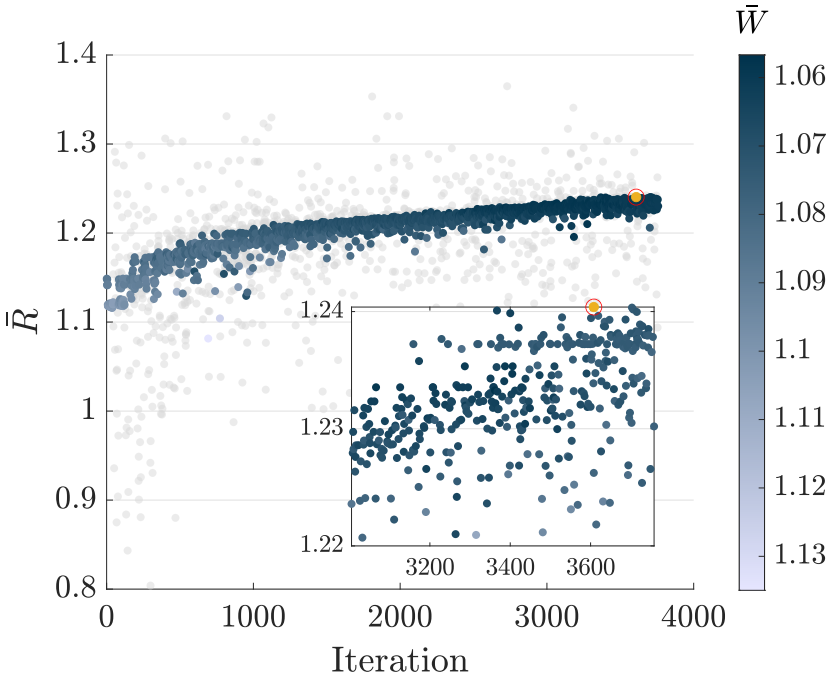

Figure 11: Objective function history: SAH configuration

[9] Attar, P. J., Tang, D., and Dowell, E. H. (2010). Nonlinear aeroelastic study for folding wing structures. *AIAA journal*, 48(10), 2187–2195.

[10] Zhao, Y. and Hu, H. (2012). Parameterized aeroelastic modeling and flutter analysis for a folding wing. *Journal of Sound and Vibration*, 331(2), 308–324.

[11] Wang, I., Gibbs, S. C., and Dowell, E. H. (2012). Aeroelastic model of multisegmented folding wings: theory and experiment. *Journal of aircraft*, 49(3), 911–921.

[12] Zhao, Y. and Hu, H. (2013). Prediction of transient responses of a folding wing during the morphing process. *Aerospace Science and Technology*, 24(1), 89–94.

[13] Conti, C., Saltari, F., Mastroddi, F., et al. (2021). Quasi-steady aeroelastic analysis of the semi-aeroelastic hinge including geometric nonlinearities. *Journal of Aircraft*, 58(5), 1168–1178.

[14] Mastracci, P., Saltari, F., Mastroddi, F., et al. (2022). Unsteady aeroelastic analysis of the semi aeroelastic hinge including local geometric nonlinearities. *AIAA Journal*, 60(5), 3147–3165.

[15] Abeyratne, R. I. R. (2014). *Law and regulation of aerodromes*, vol. 241. Springer.

[16] Nygren, C. K. P. and Schulz, M. R. R. (1996). Breguet's formulas for aircraft range & endurance an application of integral calculus. In *1996 Annual Conference*. pp. 1–90.

[17] Poloni, C., Giurgevich, A., Onesti, L., et al. (2000). Hybridization of a multi-objective genetic algorithm, a neural network and a classical optimizer for a complex design problem in fluid dynamics. *Computer Methods in Applied Mechanics and Engineering*, 186(2-4), 403–420.

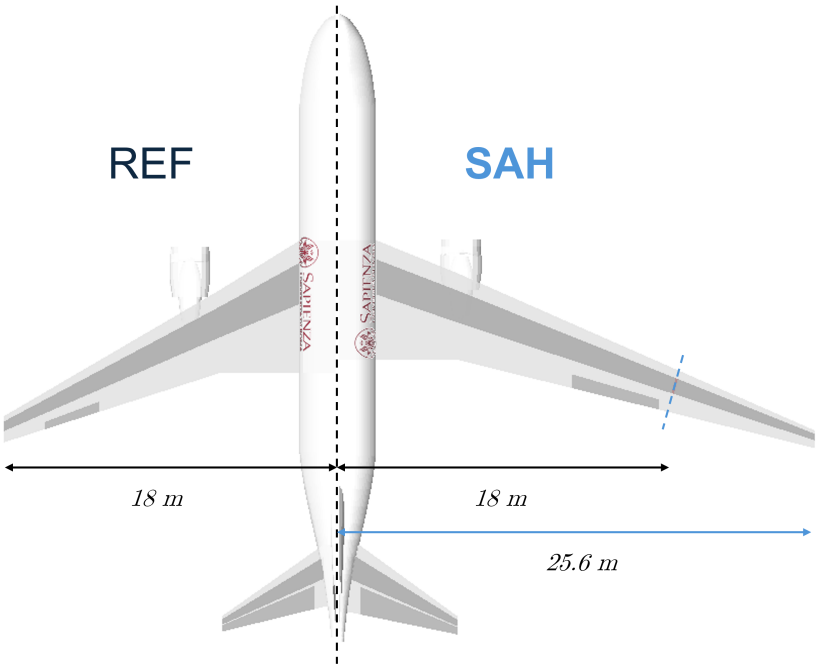

Figure 12: Geometry of aircraft with SAH compared to the optimised tip-less aircraft.

[18] Rigoni, E. and Poles, S. (2005). Nbi and moga-ii, two complementary algorithms for multi-objective optimizations. In *Dagstuhl seminar proceedings*. Schloss Dagstuhl-Leibniz-Zentrum für Informatik.

[19] Poles, S., Rigoni, E., and Robic, T. (2004). Moga-ii performance on noisy optimization problems. In *International Conference on Bioinspired Optimization Methods and their Applications, Ljubljana, Slovenia*.

[20] Albano, E. and Rodden, W. (1994). Msc/nastran aeroelastic analysis' user's guide. *MSC Software*.

[21] Hürlimann, F., Kelm, R., Dugas, M., et al. (2011). Mass estimation of transport aircraft wingbox structures with a cad/cae-based multidisciplinary process. *Aerospace Science and Technology*, 15(4), 323–333.

COPYRIGHT STATEMENT

(a) FSAH at $q_D = 10.972\,kPa$ and $n_z = 2.5$

(b) LSAH at $q_D = 5.415\,kPa$ and $n_z = 1.66$

Figure 13: Manoeuvre wing deformation and stress distribution of an aircraft with the SAH device.